A Coupling Capacitor Voltage Transformer Representation for Electromagnetic Transient Studies

D. Fernandes Jr.[1], W. L. A. Neves[1], and J. C. A. Vasconcelos[2]

(1) Departamento de Engenharia Eletrica, Universidade Federal de Campina Grande, Av. Aprigio Veloso, 882, Bodocongo, 58.109-970, Campina Grande – PB – Brazil (e-mail: damasio@dee.ufcg.edu.br, waneves@dee.ufcg.edu.br), (2) Companhia Hidro Eletrica do Sao Francisco, Rua Delmiro Gouveia, 333, Bongi, 50.761-901, Recife – PE – Brazil (e-mail: jcrabreu@chesf.gov.br)

***Abstract* – In this work, a coupling capacitor voltage transformer (CCVT) model to be used in connection with the EMTP (Electromagnetic Transients Program) is presented. A support routine was developed to compute the linear 230 kV CCVT parameters (resistances, inductances and capacitances) from the magnitude and phase of the CCVT voltage ratio measured in laboratory, from 10 Hz to 10 kHz. The errors were fairly small in the whole frequency range. The potential transformer (PT) multiple windings, its magnetic core and the silicon carbide surge arrester nonlinear characteristics were taken into account in the model in order to improve transient responses due to overvoltages. The surge arrester gap sparkover voltage was measured and the silicon carbide nonlinear characteristic was estimated. It is shown that careful attention must be taken when computing the ferroresonance suppression circuit (FSC) parameters to avoid numerical instabilities in time-domain simulations. The protection circuit is very effective in damping out transient voltages when a short circuit is cleared at the CCVT secondary side.**

Keywords – CCVT model, EMTP, system protection, data approximations.

I. Introduction

For many years, electric utilities have used coupling capacitor voltage transformers (CCVT) connected to protective relays and measuring instruments. However, problems have yet been traced to incorrect inputs. This has affected the reliability of the power system and caused failure in many CCVT. In Brazil, some electrical energy companies have reported unexpected overvoltage protective device operations in several CCVT leading to failures of some units. The reported overvoltages occurred during normal switching conditions [1].

Many works including field measurements, laboratory tests and digital simulations, have been conducted to study the performance of the CCVT. Some studies have been concentrated on nonlinear behavior of the potential transformer (PT) magnetic core to accurately simulate the transient response of CCVT [2, 3, 4].

Other works have considered the effect of stray capacitances in some CCVT elements to explain the measured frequency responses in the linear region of operation [5, 6]. There are some problems in obtaining the CCVT parameters. In [5], the used measurement techniques need disassembling the CCVT and in [6], a method was developed to estimate the CCVT linear parameters from frequency response measurements at the secondary side without the need to access its internal components. Saturation effects of the magnetic core were not taken into account.

In this work, a coupling capacitor voltage transformer model to be used in connection with the EMTP (Electromagnetic Transients Program) is presented. The potential transformer multiple windings and the silicon carbide surge arrester nonlinear characteristic were included in the CCVT model in order to improve the transient response to overvoltages. Preliminary results were presented at the IPST 2001 [7].

CHESF (Companhia Hidro Elétrica do São Francisco) made available a 230 kV CCVT unit. Frequency response measurements of magnitude and phase, in the range from 10 Hz to 10 kHz, were carried out for this unit and used as input data to a fitting routine based on Newton's method [8, 9] to compute the linear CCVT parameters R, L, C.

Digital simulations of ferroresonance were carried out using this model. The results show that careful attention must be taken when computing the ferroresonance suppression circuit (FSC) parameters to avoid numerical instabilities in time-domain simulations. The protection circuit is very effective in damping out transient voltages when a short circuit is cleared at the CCVT secondary side.

II. Basic Principles

The basic electrical diagram for a typical CCVT is shown in Fig. 1. The primary side consists of two capacitive elements C_1 and C_2 connected in series. The PT provides a secondary voltage v_o for protective relays and measuring instruments. The inductance L_c is chosen to avoid phase shifts between v_i and v_o at power frequency. However, small errors may occur due to the exciting current and the CCVT burden (Z_b) [2].

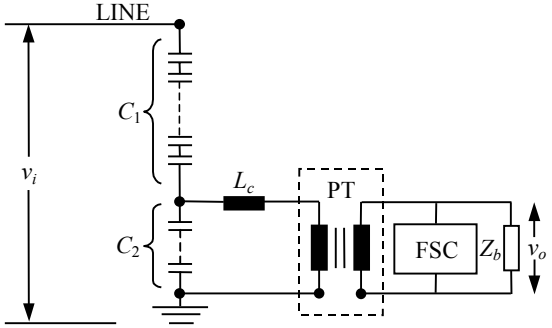

Fig. 1 Electrical diagram for a typical CCVT.

Ferroresonance oscillations may take place if the circuit capacitances resonate with the iron core nonlinear inductance. These oscillations cause undesired information transferred to the relays and measuring instruments. Therefore, a ferroresonance suppression circuit (FSC) is normally included in one of the CCVT windings.

Circuits tuned at power frequency (L in parallel with C) and a resistance to ground have been often used as ferroresonance suppression circuits [4, 6] because they damp out transient oscillations and require small amount of energy during steady-state.

III. Developed Analytical Method

The diagram shown in Fig. 1 is valid only near power frequency. A model to be applicable for frequencies up to a few kilohertz needs to take into account the PT primary winding and compensating inductor stray capacitances at least [3 – 6].

In this work, the circuit shown in Fig. 2 was used to represent the CCVT. It comprises of a capacitive column (C_1, C_2), a compensating inductor (R_c, L_c, C_c), a potential transformer (R_p, L_p, C_p, L_m, R_m) and a ferroresonance suppression circuit (R_f, L_{f1}, L_{f2}, $-M$, C_f) [5, 6].

The FSC configuration is shown in Fig. 3(a). A nonsaturable iron core inductor L_f is connected in parallel with a capacitor C_f so that the circuit is tuned to the fundamental frequency with a high Q factor [4]. The FSC digital model is shown in Fig. 3(b). The damping resistor R_f is used to attenuate oscillations caused by the ferroresonance phenomenon.

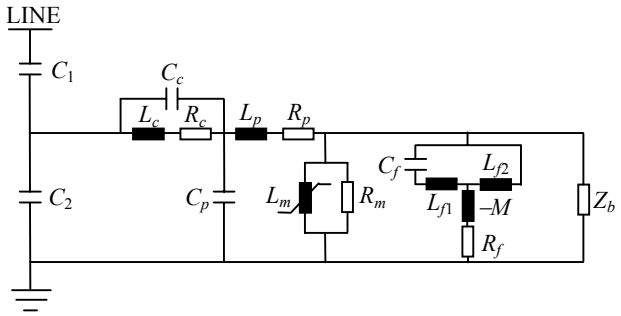

Fig. 2 CCVT model for calculation of parameters.

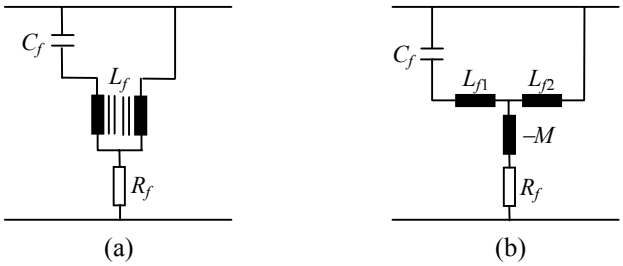

Fig. 3 (a) FSC configuration. (b) FSC digital model.

A. Calculation of the CCVT Model Parameters

In order to develop the analytical expressions of CCVT model, it was considered only the linear region of the PT magnetic core because the core was not saturated during the frequency response measurements. The nonlinearity is included in time-domain simulations to improve the representation of the transient effects in CCVT. The circuit shown in Fig. 2 is considered with specific impedances Z_1, Z_2, Z_3, Z_4, Z_5 and with all the elements referred to the PT secondary side, according to Fig. 4.

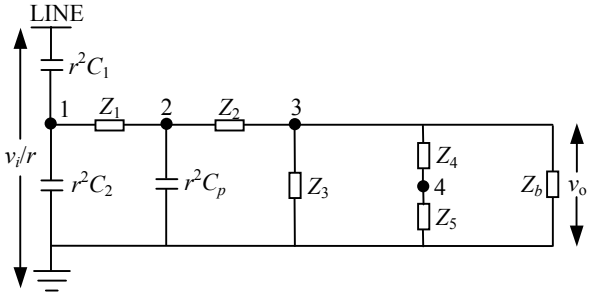

Fig. 4 CCVT model with specific impedances.

The expressions for the impedances in the s domain, with $s = j\omega$, are:

$$\begin{aligned} Z_1 &= \left[\left(R_c + sL_c\right)/r^2\right] // \left(1/r^2 sC_c\right), \\ Z_2 &= \left(R_p + sL_p\right)/r^2 ; \\ Z_3 &= \left(R_m/r^2\right) // \left(sL_m/r^2\right), \\ Z_4 &= \left(sL_{f1} + 1/sC_f\right) // \left(sL_{f2}\right), \\ Z_5 &= R_f - sM . \end{aligned} \tag{1}$$

Where, r is the PT ratio and the symbol // means that elements are in parallel.

The CCVT model parameters R, L, C should reproduce the transfer functions of magnitude and phase represented by v_o/v_i. They are calculated using the technique described below for the minimization of nonlinear functions.

B. Minimization Technique of Nonlinear Functions

Here, the used iterative technique for minimizing nonlinear functions is based on Newton's method which uses a quadratic approximation to the function $F(x)$ derived from the second-order Taylor series expansion about the point x_i. In two dimensions, the second-order Taylor series approximation can be written in the form:

$$\begin{aligned} F(x_1 + p_1, x_2 + p_2) \approx F(x_1, x_2) + \begin{bmatrix} p_1 & p_2 \end{bmatrix} \begin{bmatrix} \dfrac{\partial F(x_1, x_2)}{\partial x_1} \\ \dfrac{\partial F(x_1, x_2)}{\partial x_2} \end{bmatrix} \\ + \frac{1}{2} \begin{bmatrix} p_1 & p_2 \end{bmatrix} \begin{bmatrix} \dfrac{\partial^2 F(x_1, x_2)}{\partial x_1^2} & \dfrac{\partial^2 F(x_1, x_2)}{\partial x_1 \partial x_2} \\ \dfrac{\partial^2 F(x_1, x_2)}{\partial x_2 \partial x_1} & \dfrac{\partial^2 F(x_1, x_2)}{\partial x_2^2} \end{bmatrix} \begin{bmatrix} p_1 \\ p_2 \end{bmatrix} \end{aligned} \tag{2}$$

And for n dimension, the expression above in matrix/vector form is:

$$F(\boldsymbol{x} + \boldsymbol{p}) \approx F(\boldsymbol{x}) + \boldsymbol{p}^T \nabla F(\boldsymbol{x}) + \frac{1}{2} \boldsymbol{p}^T \nabla^2 F(\boldsymbol{x}) \boldsymbol{p} . \tag{3}$$

In order to obtain the step $\boldsymbol{p}$, the function F is minimized by forming its gradient with respect to $\boldsymbol{p}$ and setting it equal

to zero. Therefore,

$$\nabla^2 F(\boldsymbol{x})\boldsymbol{p} = -\nabla F(\boldsymbol{x}). \quad (4)$$

The approximate solution $\boldsymbol{x}_{k+1}$ is given by:

$$\boldsymbol{x}_{k+1} = \boldsymbol{x}_k + \boldsymbol{p} = \boldsymbol{x}_k - \left[\nabla^2 F(\boldsymbol{x}_k)\right]^{-1} \nabla F(\boldsymbol{x}_k). \quad (5)$$

Newton's method will converge if $[\nabla^2 F(\boldsymbol{x})]^{-1}$ is positive definite in each iterative step, that is, $z^T[\nabla^2 F(\boldsymbol{x})]^{-1} z > 0$ for all $z \neq 0$. This technique is known as the full Newton-type method [8, 9]. It is a modification of Newton's method for that iteration in which $[\nabla^2 F(\boldsymbol{x})]^{-1}$ is not positive definite. In the procedure, $\nabla^2 F(\boldsymbol{x})$ is replaced by a "nearby" positive definite matrix $\overline{\nabla}^2 F(\boldsymbol{x})$ and $\boldsymbol{p}$ is computed solving $\overline{\nabla}^2 F(\boldsymbol{x})\boldsymbol{p} = -\nabla F(\boldsymbol{x})$.

The function to be minimized is called merit function $\chi^2(\boldsymbol{x})$ and it is given by expression below:

$$\chi^2(\boldsymbol{x}) = \sum_{i=1}^{n} \left[\frac{y_i - y(\omega_i; \boldsymbol{x})}{\sigma_i} \right]^2. \quad (6)$$

Where ω_i is the i-th measured frequency value and y_i is the i-th measured frequency response value of the n data points. σ_i is the standard deviation for each y_i. $\boldsymbol{x}$ is the vector which contains the parameters R, L, C to be determined and $y(\omega_i; \boldsymbol{x})$ is the analytical model function.

A FORTRAN routine was developed to minimize the merit function $\chi^2(\boldsymbol{x})$ using the method described above. Besides the function $y(\omega_i; \boldsymbol{x})$, it is necessary to know its first and second derivatives with respect to each parameter of the vector $\boldsymbol{x}$. The algorithm is based on the following steps [7]:

1. Supply the CCVT frequency response values y_i for each frequency ω_i and enter with a guess for the parameters R, L, C (vector $\boldsymbol{x}$);
2. Determine $\chi^2(\boldsymbol{x})$ and evaluate $\chi^2(\boldsymbol{x} + \boldsymbol{p})$;
3. Save the value of $\chi^2(\boldsymbol{x} + \boldsymbol{p})$ and for a user defined number of iterations m, compare the actual value of the merit function to its old value m iterations before:
4. If the difference is greater than a user defined tolerance, go back to step 2. Otherwise, stop the iterative process.

IV. Laboratory Measurements

Frequency response measurements of magnitude and phase were carried out for the 230 kV CCVT. The rms $v - i$ nonlinear curve for the PT magnetic core was measured as well. The surge arrester nonlinear characteristic was estimated from measurements of its gap sparkover voltage in our high voltage laboratory.

A. Frequency Response Measurements

During the frequency response measurements, a low-pass filter was required to attenuate high frequency noises. A 3rd order RC active filter with a cut-off frequency of 15 kHz, was used [10]. A signal generator feeding an amplifier whose maximum peak-to-peak voltage is 2 kV, was connected across the high voltage terminal and the ground, according to Fig. 5.

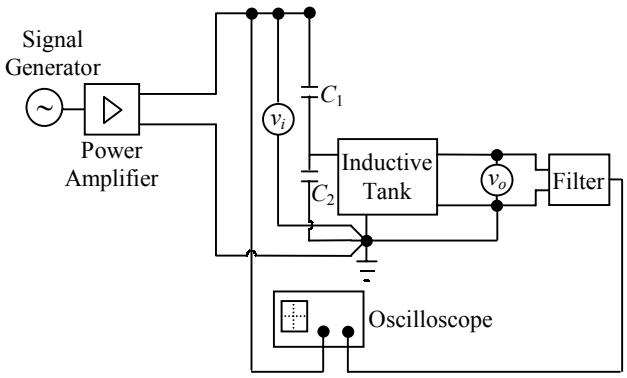

Fig. 5 Frequency response measurements for the 230 kV CCVT.

B. PT Nonlinear Characteristic Measurements

A sinusoidal voltage supplied by an autotransformer was applied across terminals $X_1 - X_3$ and gradually increased from zero up to 251.3 V rms, according to Fig. 6. The rms $V - I$ data points were obtained. The data were converted into the peak $\lambda - i$ data using a routine from [11].

In order to estimate the PT magnetic core saturation, the air core inductance was calculated by the expression:

$$L_{sat} \cong \frac{N^2 \mu_0 S}{l}. \quad (7)$$

Where, $N = 81$ is the number of coils of the secondary winding, $\mu_0 = 4\pi.10^{-7}$ H/m is the magnetic permeability in vacuum, $S = 91.5$ cm^2 is the core crossection area and $l = 71.28$ m is the average length of the secondary winding. It was considered that saturation occurs with a flux density of 2.1 T, which corresponds to $\lambda_{knee} = 1.556415$ V.s. The value of i_{knee} was calculated from [11] after a logarithmic extrapolation of the previous points in the rms $V - I$ curve. This corresponds to the previous to the last point of the λ–i data points shown in Table I. The last segment slope is L_{sat}.

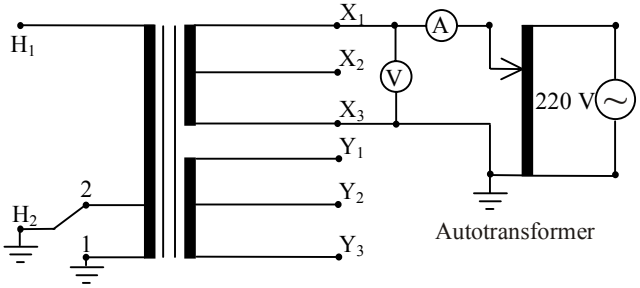

Fig. 6 Measurement of the PT saturation curve.

Table I Nonlinear characteristic of the PT magnetic core.

Peak Current (A)	Peak Flux (V.s)
0. 076368	0.025772
0.720881	0.189066
1.429369	0.396889
2.511675	0.748388
3.662012	0.863553
4.587227	0.903317
5.712037	0.942706
55.527018	1.556415
5552.7018	1.562242

C. Surge Arrester Nonlinear Characteristic Estimation

The 230 kV CCVT protection circuit comprises by a silicon carbide (SiC) surge arrester connected in parallel with the capacitance C_2.

In order to estimate the surge arrester $v - i$ characteristic, its sparkover voltage was measured at power frequency. The voltage supplied by a high voltage transformer, rated 100 kV and 10 kVA, was applied gradually across the surge arrester terminals until gap sparkover was reached. For 7 measurements, the sparkover voltage average value was 58.5 kV rms.

According to ANSI/IEEE C62.1-1989 Standard [12], for a completely assembled gapped silicon carbide arrester the power frequency sparkover voltage should not be smaller than 1.5 times the rated voltage. Therefore, the tested surge arrester was rated as a 39 kV rms unit.

A 39 kV rms surge arrester has an arrester discharge voltage (V_{10}) at 10 kA for 8/20 equal to 89.7 kV. This value of V_{10} was taken from ANSI/IEEE C62.2-1987 Standard [13].

The surge arrester $v - i$ characteristic is obtained as percent of discharge voltage at 10 kA for 8/20 μs. This characteristic depends also on the waveform applied to the arrester. In this work was considered a wavefront of 2 ms because the measurements were made at power frequency. The estimation of percent was based on a typical characteristic for 6 kV silicon carbide arrester, supplied by the manufacturer [14]. The 39 kV surge arrester nonlinear characteristic is shown in Table II.

Table II Silicon carbide surge arrester nonlinear characteristic.

Peak Current (A)	Peak Voltage (kV)
100	20.8
200	27.9
500	39.0
1000	42.9
2000	45.5

V. Analysis and Discussion of the Results

A. 230 kV CCVT Parameters

The 230 kV CCVT parameters were obtained from frequency response data points of magnitude and phase measured in the high voltage laboratory of our university. The initial guesses and fitted parameters, referred to the potential transformer secondary side, are shown in Table III and Table IV, respectively. The magnitude and phase curves for the measured and fitted voltage ratios are shown in figures 7 and 8, respectively.

Table III 230 kV CCVT initial guesses parameters.

R_c = 1.0 Ω	L_p = 3.0 mH	L_{f2} = 95.0 mH
L_c = 2.0 mH	R_m = 90.0 Ω	R_f = 4.0 Ω
C_c = 1100.0 μF	L_m = 300.0 mH	M = 10.0 mH
C_p = 1.0 μF	L_{f1} = 10.0 mH	–
R_p = 3.0 Ω	C_f = 140.0 μF	–

Table IV 230 kV CCVT calculated parameters.

R_c = 0.39 Ω	L_p = 4.92 mH	L_{f2} = 47.39 mH
L_c = 3.71 mH	R_m = 50.6 Ω	R_f = 4.99 Ω
C_c = 11486.1 μF	L_m = 700.0 mH	M = 9.31 mH
C_p = 216.3 nF	L_{f1} = 10.87 mH	–
R_p = 0.0395 Ω	C_f = 166.39 μF	–

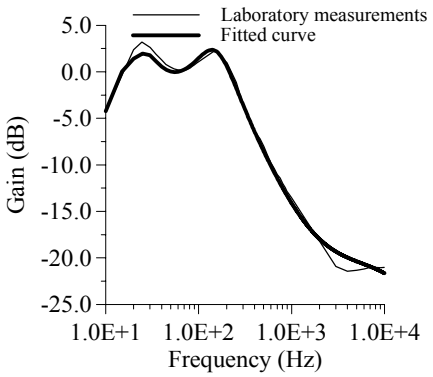

Fig. 7 Magnitude curves for the measured and fitted 230 kV CCVT voltage ratios.

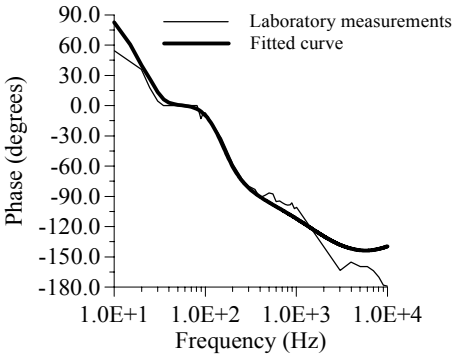

Fig. 8 Phase curves for the measured and fitted 230 kV CCVT voltage ratios.

The average errors of magnitude and phase for initial guesses parameters are, respectively, 23.3 % and 16.0°. After the fitting, the average errors of magnitude and phase are, respectively, 5.5 % and 8.9°. According to figures 7 and 8, the errors are fairly small for frequencies up to 2 kHz. Near 60 Hz the magnitude and phase errors are very small. This is the region in which the CCVT operates most of the time.

There are some CCVT parameters known at 60 Hz with reasonable accuracy, which are the cases of L_c and R_p. In the fitting process, constraints were used to perform a fine adjustment of these previously known parameters. Here they were allowed to vary within 20 %. This procedure imposes limitations for the fitting technique, but it gives more realistic results.

If C_c and C_p are neglected in the model, the frequency response of CCVT does not follow the frequency response curve of the entire model. In order to verify this, a sensitivity analysis was carried out for the voltage ratio magnitude curve, considering the entire model (parameters from Table IV) and the model using Table IV values with C_c and C_p set to zero. The results are shown in Fig. 9. It can be seen a large difference between the curves from 100 Hz onwards.

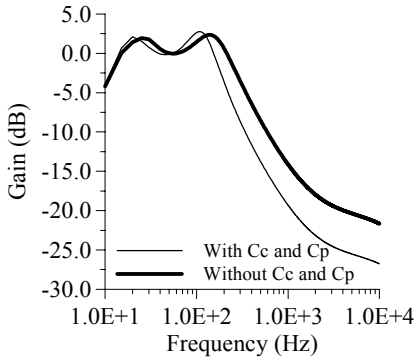

Fig. 9 Sensitivity analysis for the CCVT magnitude curve.

B. Ferroresonance Simulations

To perform the 230 kV CCVT ferroresonance simulations, MICROTRAN® [15] was used. The CCVT model is shown in Fig. 10. The magnetizing inductance L_m was replaced by a nonlinear inductance connected across the CCVT secondary terminals whose $\lambda - i$ data points are shown in Table I. The potential transformer was represented by the three winding single-phase transformer model. The protection circuit composed by a silicon carbide surge arrester was included as well. Its $v - i$ nonlinear characteristic is shown in Table II. At point A the system was represented by its Thévenin equivalent.

The ferroresonance simulations were based on tests recommended by IEC 186 Standard [16]. The first test establishes that the equipment must be energized at 1.2 p.u. of rated voltage. One of the secondary terminals is short circuited and its burden has to be nearly zero. The short circuit must be sustained during three cycles at least.

In order to analyze the importance of the FSC in transient damping, two simulations were performed: one case with the FSC included in the CCVT model and another case when the FSC is removed. In both cases, the simulations consist of a close-open operation of a switch SW connected across the CCVT secondary terminals, as shown in Fig. 10. The switch closes at t = 125 ms and remains closed during 6 cycles, when the short circuit is cleared.

In the simulation that takes into account the FSC, it was observed numerical instabilities taking place in the CCVT secondary voltage waveform, according to Fig. 11. This problem can be explained by writing the FSC admittance, $Y_f(s)$, based on its model shown in Fig 3(a).

$$Y_f(s) = \frac{1 + A_1 s^2}{B_0 + B_1 s + B_2 s^2 + B_3 s^3}. \qquad (8)$$

Where, $A_1 = C_f(L_{f1} + L_{f2})$, $B_0 = R_f$, $B_1 = L_{f2} - M$, $B_2 = R_f C_f(L_{f1} + L_{f2})$ and $B_3 = L_{f1}L_{f2}C_f - MC_f(L_{f1} + L_{f2})$. Replacing the FSC parameters by their calculated values (Table IV), it is obtained two imaginary zeroes, $z_1 = j321.18$ and $z_2 = -j321.18$, and three real poles, p_1 = 11404.0, p_2 = –577.0 and p_3 = –167.0.

The numerical instability takes place due to the pole p_1 = 11404.0 located on the right half-plane of the s plane. In order to eliminate the instability it is necessary to make B_3 in equation (8) greater than or equal to zero, assuring that all poles are located on the left half-plane of the s plane. This condition is satisfied by assuming values for inductance M smaller or equal to 8.84 mH. In fact, the fitting procedure gave a non-realizable model for the ferroresonance suppression circuit. This problem is solved if the coil L_f is divided into L_{f1} and L_{f2} and modeled as $L_1 + M$ and $L_2 + M$, respectively, where L_1 and L_2 are leakage inductances. The fitting routine was modified to take this assumption into account. The error for the amplitude curve is about the same as the fitted curve shown in Fig. 7. However, for phase curve, the fitting was not so accurate for frequencies beyond 200 Hz. Further investigations are needed regarding the CCVT equivalent circuit in order to improve the fitting for the phase curve.

For ferroresonance analysis, the value of M equal to 8.84 mH does not affect the simulation results, because the ferroresonance takes place in low frequencies, normally between 1/3 sub harmonic and the 3rd harmonic. In this frequency range the magnitude and phase curves for the CCVT voltage ratio are very similar for both values of M, 8.84 mH and the estimated value, 9.31 mH.

Fig. 12 shows the CCVT secondary voltage waveform when the FSC is removed. The oscillations remain up to 500 ms, when the steady-state is reached. Fig. 13 shows the same case with the FSC included in the CCVT model. The oscillations are damped in a time smaller than 100 ms, in conformity with ferroresonance standard tests.

Fig. 14 shows the CCVT secondary voltage when the FSC is included in the model, but considering the failure of the protection circuit. Comparing Fig. 14 with Fig. 13, one can see that the protection circuit is very effective in limiting peak transient voltages at the CCVT secondary side.

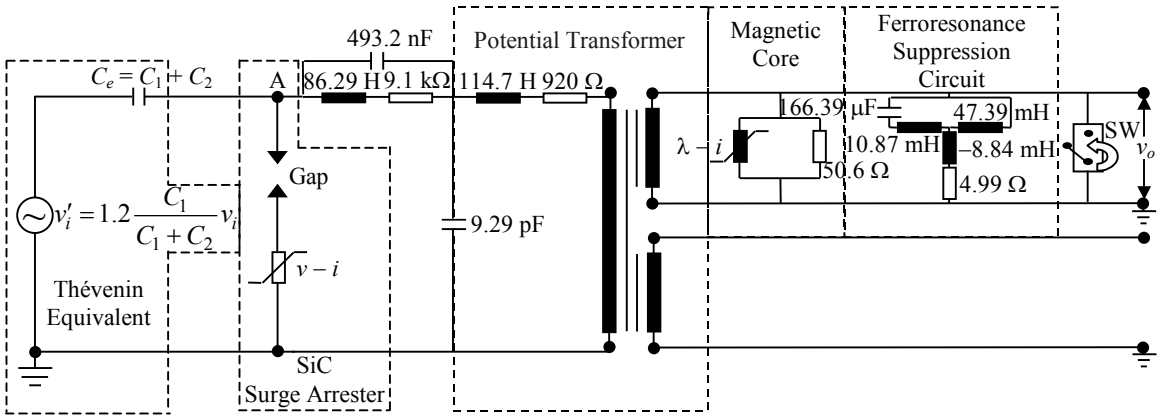

Fig. 10 230 kV CCVT model for electromagnetic transient studies.

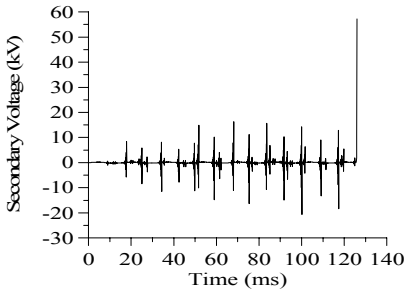

Fig. 11 CCVT secondary voltage: numerical instability.

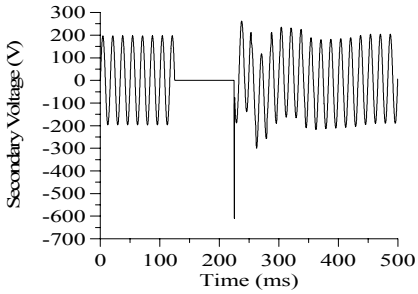

Fig. 12 Secondary voltage: CCVT without the FSC.

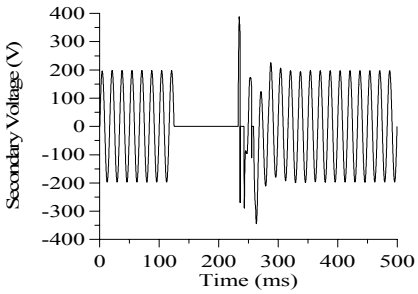

Fig. 13 Secondary voltage: CCVT with the FSC.

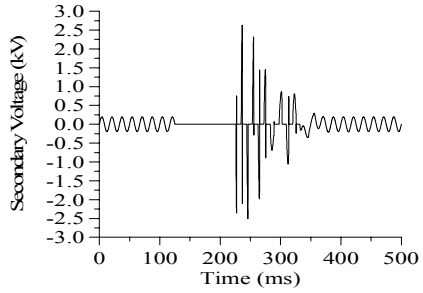

Fig. 14 CCVT secondary voltage: failure in the protection circuit.

Although the results shown in figures 11-14 are interesting, it is not certain at this stage whether they are accurate. Laboratory measurements will be carried out in the near future for validation purposes.

VI. Conclusions

In this work, a CCVT model for electromagnetic transient studies was presented. The model comprises linear parameters *R*, *L*, *C* obtained from the fitting routine based on Newton's method that uses as input data the frequency response measurements of magnitude and phase, in the range from 10 Hz to 10 kHz. The model includes the PT magnetic core and SiC surge arrester nonlinear characteristics and may be used in connection with the EMTP.

The results show that careful attention must be taken when calculating the FSC parameters to avoid numerical instabilities in time-domain simulations. Although the results reveal the importance of the FSC and the protection circuit in damping out transient voltages when a short circuit is cleared at the CCVT secondary terminals, the authors intend to perform ferroresonance tests in laboratory for validation purposes.

Acknowledgments

The authors are grateful to CHESF for providing a 230 kV CCVT unit at our laboratory. The financial support of Mr. Damasio Fernandes Jr. from the Brazilian National Research Council (CNPq) is acknowledged. The authors also wish to thank the reviewers for their suggestions.

References

[1] H. M. Moraes and J. C. A. Vasconcelos, "Overvoltages in CCVT During Switching Operations", (In Portuguese), Proceedings of the XV SNPTEE, Foz do Iguaçu, October 17-22, 1999.

[2] J. R. Lucas, P. G. McLaren, W. W. L. Keerthipala and R. P. Jayasinghe, "Improved Simulation Models for Current and Voltage Transformers in Relay Studies", IEEE Trans. on Power Delivery, Vol. 7, No. 1, pp. 152-159, January 1992.

[3] M. R. Iravani, X. Wang, I. Polishchuk, J. Ribeiro and A. Sarshar, "Digital Time-Domain Investigation of Transient Behaviour of Coupling Capacitor Voltage Transformer", IEEE Trans. on Power Delivery, Vol. 13, No. 2, pp. 622-629, April 1998.

[4] D. A. Tziouvaras, P. McLaren, G. Alexander, D. Dawson, J. Ezstergalyos, C. Fromen, M. Glinkowski, I. Hasenwinkle, M. Kezunovic, Lj. Kojovic, B. Kotheimer, R. Kuffel, J. Nordstrom, and S. Zocholl, "Mathematical Models for Current, Voltage and Coupling Capacitor Voltage Transformers", IEEE Trans. on Power Delivery, Vol. 15, No. 1, pp. 62-72, January 2000.

[5] M. Kezunovic, Lj. Kojovic, V. Skendzic, C. W. Fromen, D. R. Sevcik and S. L. Nilsson, "Digital Models of Coupling Capacitor Voltage Transformers for Protective Relay Transient Studies", IEEE Trans. on Power Delivery, Vol. 7, No. 4, pp. 1927-1935, October 1992.

[6] Lj. Kojovic, M. Kezunovic, V. Skendzic, C. W. Fromen and D. R. Sevcik, "A New Method for the CCVT Performance Analysis Using Field Measurements, Signal Processing and EMTP Modeling", IEEE Trans. on Power Delivery, Vol. 9, No. 4, pp. 1907-1915, October 1994.

[7] D. Fernandes Jr., W. L. A. Neves and J. C. A. Vasconcelos, "Identification of Parameters for Coupling Capacitor Voltage Transformers", Proceedings of the IPST 2001, pp. 463-468, Rio de Janeiro, June 24-28, 2001.

[8] D. Kahaner, C. Moler and S. Nash, *Numerical Methods and Software*, Prentice Hall PTR, New Jersey, 1989.

[9] W. H. Press, S. A. Teukolsky, W. T. Vetterling and B. P. Flannery, *Numerical Recipes in Fortran - The Art of Scientific Computing*, *Second Edition*, Cambridge University Press, 1992.

[10] D. Fernandes Jr., *Estimation of Coupling Capacitor Voltage Transformer Parameters*, M. Sc. Dissertation (In Portuguese), UFPB, September 1999.

[11] W. L. A. Neves and H. W. Dommel, "On Modeling Iron Core Nonlinearities", IEEE Trans. on Power Systems, Vol. 8, No. 2, pp. 417-423, May 1993.

[12] ANSI/IEEE Std C62.1-1989, *IEEE Standard for Gapped Silicon-Carbide Surge Arresters for AC Power Circuits*, 1989.

[13] ANSI/IEEE Std C62.2-1987, *IEEE Guide for the Application of Gapped Silicon-Carbide Surge Arresters for AC Systems*, 1987.

[14] IEEE Surge Protective Devices Committee, "Modeling of Current-Limiting Surge Arresters", IEEE Trans. on Power Apparatus and Systems, Vol. PAS-100, No. 8, pp. 4033-4040, August 1981.

[15] Microtran Power System Analysis Corporation, *Electromagnetic Transients Analysis Program*, Vancouver, 1999.

[16] IEC 186 (1969), *Voltage Transformers*, First Supplement (1970), Amendment No. 1, 1978.